Hierarchical simulations for the design of supertough nanofibers inspired by spider silk

Federico Bosia,[1,*] Markus J. Buehler,[2,3,†] and Nicola M. Pugno[2,3,4,5,‡]

[1]*Department of Theoretical Physics, Università di Torino, Via Pietro Giuria 1, 10125 Torino, Italy*

[2]*Laboratory for Atomistic and Molecular Mechanics, Department of Civil and Environmental Engineering, Massachusetts Institute of Technology, 77 Massachusetts Avenue, Room 1-235A&B, Cambridge, Massachusetts 02139, USA*

[3]*Laboratory of Bio-inspired Nanomechanics "Giuseppe Maria Pugno", Department of Structural and Geotechnical Engineering, Politecnico di Torino, Corso Duca degli Abruzzi 24, 10129 Torino, Italy*

[4]*National Institute of Nuclear Physics, National Laboratories of Frascati, Via E. Fermi 40, 00044, Frascati, Italy*

[5]*National Institute of Metrological Research, Strada dell Cacce 91, I-10135, Torino, Italy*

(Received 23 March 2010; revised manuscript received 7 September 2010; published 3 November 2010; corrected 9 November 2010)

Biological materials such as spider silk display hierarchical structures, from nano to macro, effectively linking nanoscale constituents to larger-scale functional material properties. Here, we develop a model that is capable of determining the strength and toughness of elastic-plastic composites from the properties, percentages, and arrangement of its constituents, and of estimating the corresponding dissipated energy during damage progression, in crack-opening control. Specifically, we adopt a fiber bundle model approach with a hierarchical multiscale self-similar procedure which enables to span various orders of magnitude in size and to explicitly take into account the hierarchical topology of natural materials. Hierarchical architectures and self-consistent energy dissipation mechanisms (including plasticity), both omitted in common fiber bundle models, are fully considered in our model. By considering one of the toughest known materials today as an example application, a synthetic fiber composed of single-walled carbon nanotubes and polyvinyl alcohol gel, we compute strength and specific energy absorption values that are consistent with those experimentally observed. Our calculations are capable of predicting these values solely based on the properties of the constituent materials and knowledge of the structural multiscale topology. Due to the crack-opening control nature of the simulations, it is also possible to derive a critical minimal percentage of plastic component needed to avoid catastrophic behavior of the material. These results suggest that the model is capable of helping in the design of new supertough materials.

DOI: 10.1103/PhysRevE.82.056103 PACS number(s): 61.46.−w, 07.05.Tp, 62.25.Mn

I. INTRODUCTION

Spider silk is one the toughest materials known in nature. It is extremely ductile and able to stretch up to 50% of its length without breaking, due to its secondary bond breaking [1,2] and its complex hierarchical architecture [3–5]. These properties give it a very high toughness, or specific work to fracture (on the order of 170 J/g), which equals that of commercial polyaramid (aromatic nylon) filaments, which are benchmarks of modern polymer fiber technology. Simultaneously, its tensile strength is superior to that of high-strength steel and as strong as aramid filaments, such as Kevlar. Only recently, with the advent of nanotubes, carbon nanotubes/polyvinyl alcohol gel composites have been produced by Baughman's group [6], where such composites display a huge work to fracture per unit mass (570 J/g), about three times larger than that of natural spider silk, thus resembling a form of synthetic spider silk. Such supertoughness is needed for producing novel nanotechnology-based tissues. To illustrate the significance of this value (570 J/g) it is sufficient to consider that such a synthetic spider web (with a density of about 1300 kg/m^3) composed of 100 radial silks, 100 m in length, and 1 cm in radius would be sufficient to stop a Boeing-747 (with a mass of 180 tons and a velocity of 800 km/h). Similar strength and toughness values have been recently obtained with materials based on nanotube based ribbons [7], fibers [8], composites [9], yarns [10], sheets [11], films [12], and others.

In general, biological materials and structures have been thoroughly studied to mimic their fascinating properties, e.g., the strength and toughness of nacre, bone, and dentine [13] or the smart adhesion of spiders and geckos, also envisioning "Spiderman" suits [14], with the related size-scale problems, from spider to man. In general, various length scales are needed to model full-size structures starting from the constituent nanostructures. To address this issue, we have developed a hierarchical fiber bundle model (HFBM) [15–17] as an extension of the classical fiber bundle models (FBMs) [18–21], which have been extensively studied during the past years. These models consist of a set ("bundle") of parallel fibers having statistically distributed strengths, loaded parallel to the fiber direction, and in which after each fiber failure the load is redistributed among the intact ones. In spite of their simplicity, these models can often capture the most important aspects of material damage. In some cases, FBMs can also include different fiber types [18], effects of fiber slack [22], and plasticity [23–25] to model microscale ductile mechanisms [26,27]. In many cases, important analytical results have been obtained for the mechanical quantities of interest, including asymptotic failure distributions [28]. This type of modeling has also been extended to twisted fiber

*fbosia@to.infn.it

†mbuehler@mit.edu

‡Corresponding author. FAX: (+39) 011 5644899; nicola.pugno@polito.it

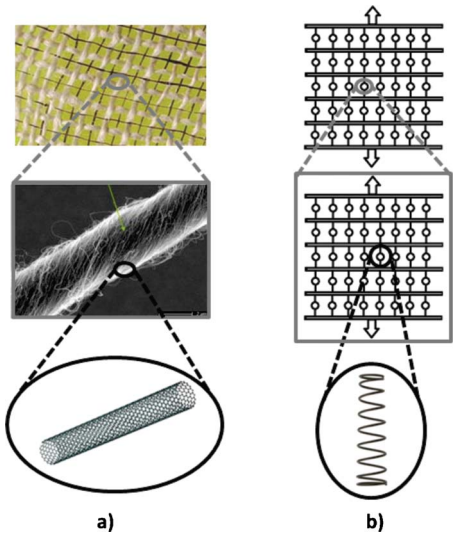

FIG. 1. (Color online) (a) Hierarchical structure of a nanotube composite: single nanotubes are spun into bundles forming micrometer-scale fibers, which in turn can be used to form structures like textiles (images are taken from [6,11]); (b) corresponding HFBM modelization in two levels: the nanotube corresponds to a fiber (or "spring") in a bundle, in turn representing a fiber in a second-level bundle. Arrows represent loading directions.

bundles [29] in order to better model ribbon- or yarn-type systems. One earlier application of a HFBM by the authors was the calculation of the space elevator cable strength [15,16], including the role of defects, previously thoroughly investigated in different systems both theoretically [30], experimentally [31], and with atomistic [32] or continuum [33] simulations.

Analytical and numerical studies also exist in the literature on the scaling of strength with size in brittle or viscoelastic matrix fibrous composites [34]. Here, we use a HBFM approach to model the plastic as well as the fracture behavior of large-scale nanocomposites such as those mentioned above, with the aim of providing a numerical tool to design tailor-made properties [12], e.g., by changing the plastic fiber content. Accordingly, in this work, we introduce plasticity in the HFBM. Fixing our attention on one of the toughest materials known today [6], a synthetic spider silk composed of single-walled carbon nanotubes (60% in weight) and polyvinyl alcohol gel (40%), we compute strength and specific energy absorption of $\sigma=1.9$ GPa and $E=583$ J/g, comparable to those experimentally observed of $\sigma=1.8$ GPa and $E=570$ J/g. The results suggest that our code is ideal to design *in silico* new supertough materials, with different plastic or brittle fiber contents, e.g., to avoid a catastrophic behavior in the material stress-strain response.

Figure 1 shows the overall geometry of the systems considered here and the hierarchical approach used to span various orders of magnitude in length: single nanotubes are modeled as fibers, nanotubes spun into (composite) fibers are modeled as fiber bundles, and larger-scale structures such as nanotube-based textiles can be modeled through higher-order fiber bundles, whose constituent fibers derive their properties from the lower level fiber bundles.

In this paper, we specifically focus on the following questions: (1) Can we model the behavior (e.g., strength and toughness) of the above discussed nanotube-based composites using a HFBM, starting from the properties and volume fractions of the constituents (including plastic matrix or fibers)? (2) How does the mechanical behavior and energy dissipation vary as functions of plastic fiber content? (3) What is the scaling behavior of these properties with specimen dimensions? These questions are addressed in the following sections.

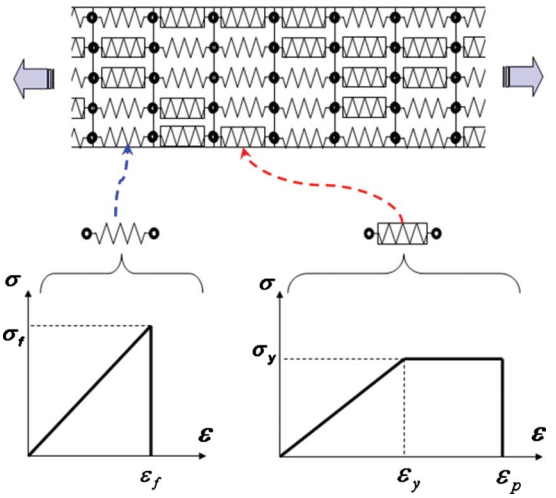

FIG. 2. (Color online) Schematic representation of the mixed fragile-plastic fiber bundle model; constitutive laws are shown for fragile (left) and plastic (right) fibers, respectively. In the case of the composite under consideration, $\sigma_f=34$ GPa, $\sigma_y=70$ MPa, $\varepsilon_p=2$, and Young's moduli are $E_f=1$ TPa and $E_p=2$ GPa.

II. SIMULATION MODEL

The model used here is related to that proposed by Pugno [15], described in detail by Bosia *et al.* [17] and Pugno *et al.* [16]. It is based on an equal-load-sharing (ELS) FBM approach, replicated in a hierarchical scheme at various length scales ("levels") to predict from statistical considerations the mechanical behavior of full-length nanotube-based bundles, starting from the statistical properties at nanoscale. Other possibilities exist for the choice of the type of FBM at single level, e.g., local-load sharing (LLS) [35,36] or global-load sharing, including friction in the case of twisted bundles [29]. We choose to adopt the simplest possible model at single level, i.e., ELS, in order to evaluate the predictive capabilities of the hierarchical approach. For the same reason, another approximation is adopted in the present approach, i.e., the nanotube composite is modeled by simply assuming that the fibers of each FBM bundle can assume different mechanical properties and constitutive laws, and in particular they can be assigned perfectly brittle or ductile behavior (Fig. 2). This amounts to neglecting to explicitly introduce shear effects in the viscoelastic matrix, which provides load transfer between nanotubes (see, e.g., [37–39] for an in depth analysis of this issue). Despite these rather radical approximations at single level, the validity of the approach can be confirmed by comparison with experimental results (see Sec. III).

Thus, the modeled specimen consists, at level 1, of a chain of bundles of fibers having either perfectly brittle or plastic behavior. The overall percentage of plastic fibers in the specimen is determined by the "plastic" parameter p that varies between 0 (100% brittle fiber content) and 1 (100% plastic fiber content). Both types of fibers are randomly distributed in the specimen. Brittle fibers are characterized by a Young's modulus E_f, length l_f, cross-sectional area A_f, and Weibull-distributed fracture strengths σ_{fij}, with size parameter σ_{0f} (nominal failure stress) and shape parameter m_f (Weibull modulus). Plastic fibers are characterized by a Young's modulus E_p, length l_p, cross-sectional area A_p, Weibull-distributed yield strengths σ_{yij} around the nominal value σ_{0y} with Weibull modulus m_y, and Weibull-distributed ultimate strains ε_{pij} around the nominal value ε_{0p} with Weibull modulus m_p. This is illustrated in Fig. 2, where the stress-strain behavior for single fibers is shown. Fragile and plastic fibers then combine in forming bundles and chains of bundles, with complex mechanical behavior emerging from that of the constituent fibers. The presence of defects in the structure at nanoscale or microscale is also accounted for, as described by Pugno *et al.* [16], and these are introduced as a chosen percentage of randomly distributed voids (i.e., fibers whose rigidity is set to zero) in the chain of bundles arrangement.

The specimen's stress-strain behavior is determined by imposing an increasing external stress and "rupturing" individual fibers in the bundle in successive steps. This is done by setting at each fracture event the imposed external stress and strain to those necessary to fracture the "weakest" fiber in the bundle, according to its failure parameters. This amounts to carrying out quasistatic loading simulations in crack-opening control, with the possibility of obtaining regions of the stress-strain curve where stresses and strains simultaneously decrease, despite the increase in damage level. This feature of the model is important because it allows us to correctly estimate the dissipated energy, and therefore specimen toughness, as discussed below and is therefore included in all simulations. After each fracture event, the load is redistributed uniformly among the fibers in the same section of the fractured one. While in the case of a bundle of brittle fibers the problem reduces to the calculation of successive elastic equilibrium states in a variable number of springs arranged in series and in parallel, the introduction of ductile fibers causes the problem to become nonlinear and load-history dependent, because one must account for nondisappearing plastic stresses for yielded fibers and hysteresis (i.e., yielded fibers have a linear elastic behavior for decreasing strains and plastic behavior for increasing strains), and therefore the numerical procedure is more cumbersome. Since the fiber failure and yield strengths are assigned randomly according to the Weibull distribution, results differ for each simulation, and average trends can be derived from repeated simulations.

Hierarchy is implemented as described by Pugno *et al.* [16] and Bosia *et al.* [17], the input mechanical behavior of a level 2 "fiber" or subvolume is statistically inferred from the output deriving from thousands of level 1 simulations, that of a level 3 fiber from level 2 simulations, and so on. Specifically, level 1 simulations provide Young's modulus, yield strength, and ultimate strain values for level 2 subvolumes, all of which are considered to have the more general plastic behavior, as do level 3 subvolumes and above. Brittle behavior is therefore introduced explicitly only in the level 1 bundle.

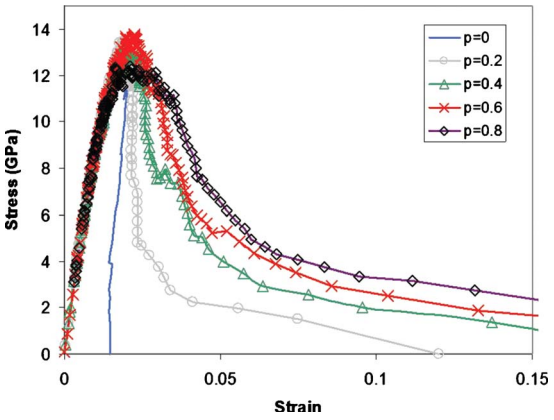

FIG. 3. (Color online) Typical level 1 stress-strain curves for varying plastic fiber percentage p (see text for details). The catastrophic behavior (softening with positive slope, $p=0$) disappears for about $p>0.2$.

Overall, the nanocomposite is modeled as a $N_{xk}\times N_{yk}$ ensemble of subvolumes arranged in a chain of bundles. Each of these subvolumes is in turn constituted by $N_{x(k-1)}\times N_{y(k-1)}$ subvolumes, arranged in a chain of bundles as before. This scheme is applied for k "generations," down to a level 1 subvolume, which is constituted by a $N_{x1}\times N_{y1}$ arrangement of fragile or plastic fibers, representing the actual nanoscale fibers (e.g., carbon nanotubes) or the plastic constituent (e.g., polyvinyl alcohol gel), respectively. A scale-invariant approach is adopted, whereby the simulated structure appears the same at any given scale level (i.e., the length/width ratio is constant), and therefore $N_{x1}=N_{x2}=\cdots=N_{xk}=N_x$ and $N_{y1}=N_{y2}=\cdots=N_{yk}=N_y$. Overall, the nanocomposite is therefore constituted by a total number of fibers given by $N_{tot}=(N_xN_y)^k$, where k is the chosen number of levels.

Simulations are carried out in what amounts to the numerical equivalent of crack-opening displacement control, i.e., the simulation proceeds by fracturing one fiber at a time, based on the respective yield or fracture strengths and the stresses acting on the fibers, and then setting the overall stress and strain to the appropriate values. This gives rise to stress-strain curves as those pictured in Fig. 3, which include "softening" phases with receding stresses and/or strains. The corresponding branches can be captured experimentally only by controlling a monotonically increasing variable (e.g., the softening with negative slope by controlling the strain), and thus the softening with positive slope (curve for $p=0$) can be observed only controlling the crack opening; accordingly, also controlling the strain would lead to an undesired catastrophic failure of the specimen [40].

Energetic aspects of the simulated tensile tests are also accounted for. At each level, variations in external work ΔW, accumulated elastic energy ΔU, and dissipated energy $\Delta\Omega$ (in plastic deformation and crack surface formation) are

computed for each fiber failure. The external work ΔW is given by

$$\Delta W = F\Delta x + x\Delta F, \tag{1}$$

where F and x are the applied force and displacement, respectively, and ΔF and Δx are their variations at the considered loading step. The accumulated elastic energy ΔU is given by

$$\Delta U = \tfrac{1}{2}x^2\Delta k + kx\Delta x, \tag{2}$$

where Δk is the variation in the overall bundle rigidity due to the fracture or yielding of the relevant fiber. As mentioned above, the dissipated energy is composed of a contribution due to fragile fiber failure and a contribution due to the deformation of yielded plastic fibers:

$$\Delta\Omega = (G_C A_f)_{fragile} + A_f l_f \Big(\sum_j \sigma_{yj}|\Delta\varepsilon_j|\Big)_{plastic}, \tag{3}$$

where G_C is the material fracture energy, A_f is the fiber cross-sectional area, l_f is the length, σ_{yj} is the yield stress of the jth yielded fiber, $\Delta\varepsilon_j$ is the variation in its strain, and the sum is carried out over yielded fibers only. Finally, energy balance considerations allow the determination of the variation in the released kinetic energy ΔT (e.g., in stress waves and acoustic emissions) as

$$\Delta T = \Delta W - \Delta U - \Delta\Omega. \tag{4}$$

III. RESULTS

A. Single level results

First, we evaluate the qualitative behavior of the proposed model. One of the possible applications is to evaluate the influence of the relative volume fractions of the components on the mechanical behavior of a carbon nanotube-based composite. This is of practical importance for the design of composites with tailor-made properties, as is often required in materials science.

To do this, the influence of the percentile content of plastic fibers in the composite specimen can be investigated, i.e., the dependence on the parameter p. We initially set for simplicity $l_f = l_p = 100$ nm, $A_f = A_p = 8 \times 10^{-1}$ nm^2, $E_f = E_p = 1$ TPa, $\sigma_{0f} = \sigma_{0y} = 30$ GPa, $\varepsilon_{0p} = 0.1$, $N_{x1} = 100$, $N_{y1} = 100$, and consider only a single simulation level. The previous values model a nanotube composite bundle. The parameter p is made to vary between 0 and 1, i.e., the model specimen varies between a perfectly fragile and a perfectly plastic behavior, respectively. Simulations are replicated typically 1000 times to derive reliable statistics.

Typical stress-strain results for a single representative run are shown in Fig. 3 for $m_f = m_p = 2$. It is interesting to notice that in the case of 100% fragile fibers, the specimen fractures after a softening phase with positive slope. This corresponds to a catastrophic behavior, i.e., controlling force or displacement would result in an abrupt failure with large emission of kinetic energy. This undesired effect does not occur when approximately 20% of plastic fibers are present. While there is little effect on the overall strength of the model specimen, failure strains increase considerably with increasing p. It is therefore clear that an increasing percentage of plastic fibers implies a greater energy dissipation. This is due to the fact that plastic fibers continue to support stresses after yielding, and therefore continue to dissipate energy when fragile fibers would have ceased to. This effect is particularly interesting for engineering applications, where a considerable energy as well as stress is required to bring a specimen to failure. The effect is indeed exploited in carbon nanotube-based composites, modeling the behavior seen in nature, e.g., in the case of spider silk.

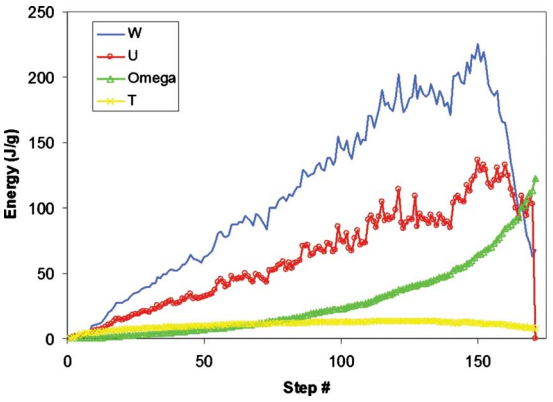

FIG. 4. (Color online) Example of energetic analysis for a level 1 simulation up to specimen failure: variation of external work (W), potential elastic energy (U), dissipated energy (Ω=Omega), and released energy (T) as a function of simulation step number. All energies are expressed per unit mass (in grams).

Figure 4 illustrates the variation of external work W, elastic energy U, dissipated energy Ω, and released energy T for a typical simulation with $p=0.4$. Again, for $m_f = m_p = 2$. It must be stressed that the abscissas do not correspond to time, as one would have in a displacement- or force-controlled experiment, and rather to a simulation step that corresponds to the failure or yielding of a single fiber composing the chain of bundles. It is noticeable that the external work carried out to deform the specimen is only partially accumulated in elastic energy in the specimen or dissipated due to crack surface formation or plastic deformation. This means that at each fiber fracture part of the remaining energy is released in the form of stress waves. As the simulation advances and more and more plastic fibers reach their yield point, the dissipated energy becomes proportionally more significant, leading to a decrease in released energy. The final part of the simulation, with decreasing W and U, corresponds to the softening branch of the stress-strain curve. Analysis of the scaling behavior of the released and dissipated energy bursts in these simulations highlights power laws, in accordance with previous works in the literature in cases of an ELS FBM [41] and of a fuse model [42]. This type of study was also previously carried out for the present HFBM with brittle fibers only [43] and power-law scaling also found for released and dissipated energies, with scaling exponent values similar to those expected from the asymptotic "universal power law $E^{-5/2}$" [41]. The same power-law scaling is found for the

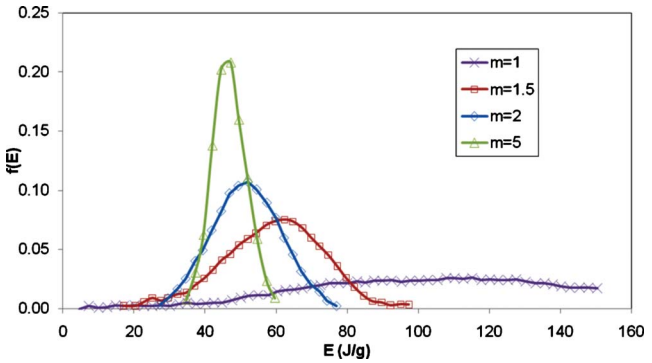

FIG. 5. (Color online) Energy-to-break (per unit mass) E distributions for varying values of m (modulus for the Weibull distribution of fiber strengths). f is the relative frequency of the energy-to-break value for a given m.

present elastoplastic FBM, with and additional dependency of the scaling exponent from the "plastic" parameter p.

The influence of the Weibull modulus parameters m_f and m_y on the energy-to-break, i.e., the energy that it is necessary to provide to the system in order to achieve specimen failure, is also evaluated for the system considered previously. Once again, a single simulation level is considered to highlight parameter dependence, and the resulting energy-to-break distributions are shown in Fig. 5. As either (or both) of the Weibull moduli increase, the energy-to-break distribution becomes narrower and the peak shifts toward smaller values. This is to be expected, as greater modulus values correspond to narrower more peaked fiber strength distributions. These parameters can be used to fit experimental data for various known systems. Results for bundle strength are qualitatively similar, i.e., Gaussian-like distributions with decreasing width for increasing Weibull modulus values.

Next, we evaluate the influence of the p parameter on the strength and toughness of the specimen for a single simulation level. Results from simulations are shown in Fig. 6, where all numerical points are fitted with second-order polynomials. Three cases are considered: (1) fragile and plastic fibers with $E_f=E_p$ and $\sigma_{0f}=\sigma_{0y}$, (2) fragile and plastic fibers with $E_f=2E_p$ and $\sigma_{0f}=2\sigma_{0y}$, and (3) fragile and plastic fibers with $E_f=10E_p$ and $\sigma_{0f}=10\sigma_{0y}$. In the first case, specimen strength remains unvaried with p, while the toughness increases considerably (about eight times from $p=0$ to $p=0.9$). In the second and third cases, the specimen strength decreases with p, while toughness increases. As is intuitive, the strength variation is proportional to the ratio between the strengths of the two types of fibers. The toughness variation, on the other hand, does not follow an equally simple law. This shows how, based on the properties of the constituent fibers, a composite may be designed with the required

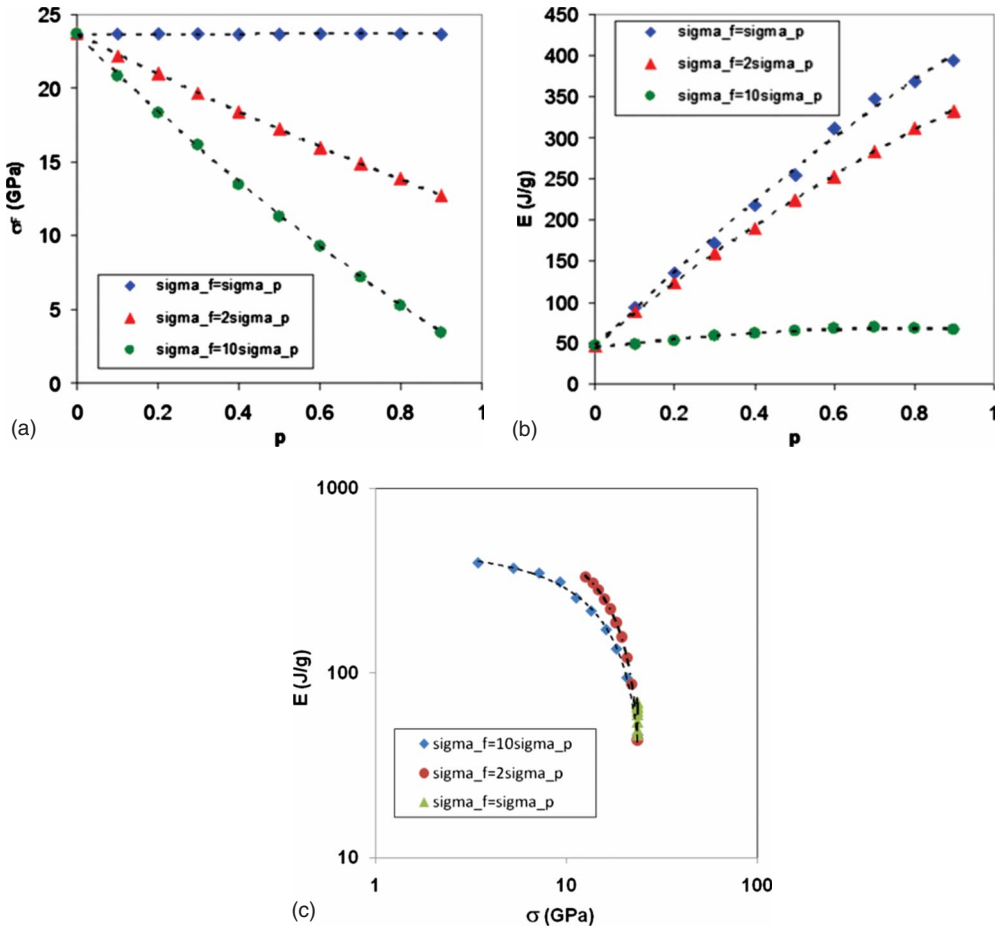

FIG. 6. (Color online) Numerically calculated dependence of (a) specimen strength σ_f and (b) energy-to-break (per unit mass) E on the parameter p; (c) corresponding energy-to-break vs strength plot. Numerical points are fitted with second-order polynomials.

strength and toughness characteristics. Often, a compromise between the two desirable characteristics needs to be reached. This is highlighted by including the data from Figs. 6(a) and 6(b) in a single strength vs energy-to-break (log-log) plot in Fig. 6(c), which shows the typical inverse-proportional behavior encountered for the overwhelming majority of structural materials [5].

B. Hierarchical multilevel results

To test the predictive capabilities of the proposed model, we choose to analyze a carbon nanotube-based composite of particular interest, recently studied by Baughman's group [6]. In this work, 100-m-long 50-μm-wide fibers are spun, containing single-walled carbon nanotubes (60% in weight) and polyvinyl alcohol gel (40%). This 100 m composite fiber is experimentally found to simultaneously have an extremely high strength (1.8 GPa) and energy-to-break (up to 570 J/g), resembling synthetic spider silk superfibers. In fact, the authors noted that the last value exceeds those for any known natural or synthetic fiber, including the spider silk. This toughness is due to a combination of high strength and high strain to failure.

In this composite, the carbon nanotubes are effectively arranged in bundles, so that a FBM approach is justified. Thus, the material can be modeled using the approach described in Sec. II. To verify the validity of the model, numerical results can be compared to experimental values. Additionally, numerical simulations can be of help to evaluate the mechanical behavior of "virtual" composites similar to the one considered here, obtained by varying component properties or volume fractions.

A multilevel approach is adopted to cover the length span from nanotube length to full-size fiber (from hundreds of nanometers to a hundred meters) composed of nanotubes and polyvinyl alcohol gel ($p=0.4$). We thus use for the carbon nanotubes $l_f=l_p=10^{-7}$ nm, $A_f=A_p=0.785$ nm^2, and $E_f=1$ TPa, whereas for the polyvinyl alcohol gel we use $E_p=2$ GPa, $\sigma_{0f}=34$ GPa, $\sigma_{0y}=70$ MPa, and $\varepsilon_{0p}=2$. Note that the density of both the components is close to 1300 kg/m^3 (the value that we have assumed to compute the energy per unit mass). The overall length and cross section of the fiber are $L=100$ m and $A=1.96$ μm^2, respectively. Using a scale-invariant approach, whereby the simulated structure appears the same at any given scale level (i.e., the length/width ratio is constant), we have $N_{x1}=N_{x2}=\cdots=N_{xk}$ and $N_{y1}=N_{y2}=\cdots=N_{yk}$, and it is therefore possible to model the composite using $k=4$ levels, with $N_x=178$ and $N_y=224$.

Figure 7 shows the resulting simulated stress and energy absorption as functions of strain for the considered fiber and Weibull modulus values of $m_f=m_y=1.5$. The calculated strength and energy-to-break are $\sigma=1.86$ GPa and $E=582.73$ J/g, respectively. These values and the numerical curves shown in the figure compare well with experimental data (see supplementary information by Dalton *et al.* [6]; $\sigma=1.8$ GPa and $E=570$ J/g). An even better correspondence could probably be obtained by assuming strain hardening instead of perfectly plastic behavior for plastic fibers in our simulations; however this would complicate the model somewhat and add further fitting parameters, whereas the aim of this work is to provide as simple a model as possible to quantitatively reproduce the observed behavior.

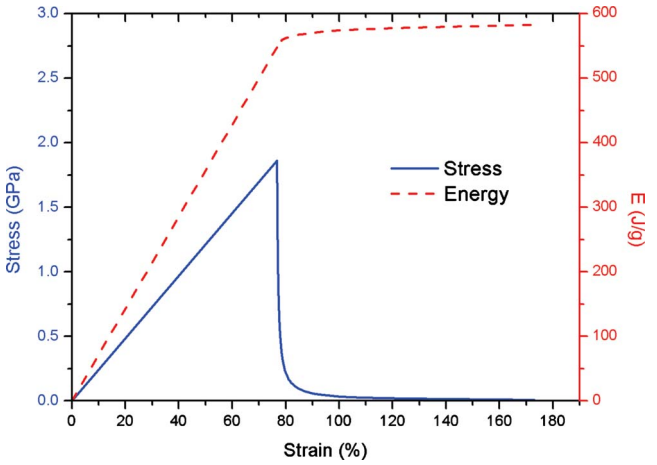

FIG. 7. (Color online) Stress-strain behavior and energy dissipated, based on multilevel simulations, of a 100-m-long synthetic spider silk strand made with carbon nanotube composite fiber. Our predictions of a strength of $\sigma=1.9$ GPa and dissipated energy of $E=583$ J/g are comparable to those experimentally observed of $\sigma=1.8$ GPa and $E=570$ J/g.

To highlight the scaling of specimen strength, the numerically calculated values obtained at each of the k levels are plotted in Fig. 8. As an example, a 10% uniformly distributed defect content is considered. The presence of defects contributes on average to a 14% decrease in fiber strength over the size scales involved. This effect is not present in the ideal case of a nondefective fiber. In this case, a two-level simulation is sufficient to determine full-length structure properties. Similar results are obtained for carbon nanotube composite fiber toughness and stiffness.

IV. CONCLUSION

We presented a HFBM simulation approach which includes brittle and plastic fibers to simulate the behavior of

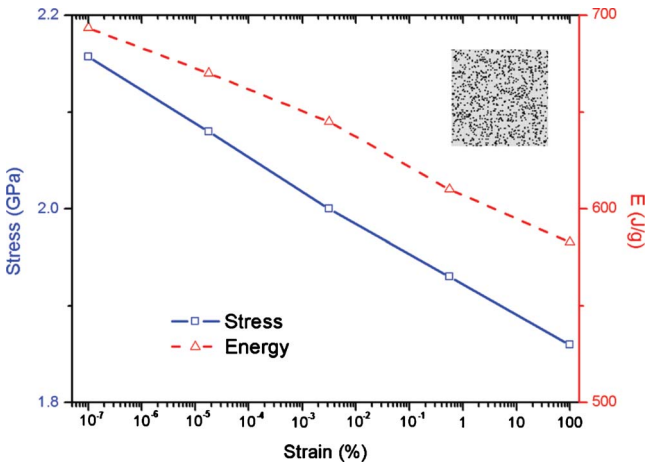

FIG. 8. (Color online) Simulated scaling of specimen strength and absorbed energy for the considered carbon nanotube based composite fiber for a 10% defect concentration. Inset: defect "map" of a section of the specimen, with defects shown as dark dots.

full-scale spider-silk-inspired fibers. The model has good predictive capabilities, and comparison with experimental results regarding nanotube fibers with exceptional toughness and high strength yields good agreement between numerical and experimental results. This model could be used to aid in the design of supercomposites materials with tailor-made properties, based on the chosen constituents and their relative mass percentage. Our results indicate that the formation of hierarchies play a crucial role in achieving superior mechanical traits and provide the means to optimize the performance of nanostructured materials. This suggests that the use of theoretical and numerical models could be essential to prepare the way for new synthetic materials, and our findings may enable the development of self-assembled bioinspired nanomaterials based on a variety of tailored building blocks. Future studies could be specifically focused on hierarchical biological materials or include molecular-dynamics simulations to extract fundamental material parameters for use in our model.

ACKNOWLEDGMENTS

M.J.B. acknowledges support by the Army Research Office (grant no. W911NF-06-1-0291), a MURI award (grant no. W911NF-09-1-0541), and the Air Force Office of Scientific Research (grant no. FA9550-08-1-0321). N.M.P. acknowledges support by the Metrology on a cellular and macromolecular scale for regenerative medicine-METREGEN (2009–2012) grant. Support from the MIT-Italy program (MITOR) is greatly acknowledged.

[1] B. L. Smith *et al.*, Nature (London) **399**, 761 (1999).
[2] T. Ackbarow and M. J. Buehler, Nanotechnology **20**, 075103 (2009).
[3] H. J. Zhou and Y. Zhang, Phys. Rev. Lett. **94**, 028104 (2005).
[4] S. Keten and M. J. Buehler, Nano Lett. **8**, 743 (2008).
[5] Z. Qin, S. Cranford, T. Ackbarow, and M. J. Buehler, Int. J. App. Mech. **1**, 85 (2009).
[6] A. B. Dalton, S. Collins, E. Munoz, J. M. Razal, V. H. Ebron, J. P. Ferraris, J. N. Coleman, B. G. Kim, and R. H. Baughman, Nature (London) **423**, 703 (2003).
[7] B. Vigolo, A. Penicaud, C. Coulon, C. Sauder, R. Pailler, C. Journet, P. Bernier, and P. Poulin, Science **290**, 1331 (2000).
[8] P. Miaudet, S. Badaire, M. Maugey, A. Derre, V. Pichot, P. Launois, P. Poulin, and C. Zakri, Nano Lett. **5**, 2212 (2005).
[9] P. Miaudet, A. Derre, M. Maugey, C. Zakri, P. M. Piccione, R. Inoubli, and P. Poulin, Science **318**, 1294 (2007).
[10] M. Zhang, K. R. Atkinson, and R. H. Baughman, Science **306**, 1358 (2004).
[11] M. Zhang, S. L. Fang, A. A. Zakhidov, S. B. Lee, A. E. Aliev, C. D. Williams, K. R. Atkinson, and R. H. Baughman, Science **309**, 1215 (2005).
[12] F. M. Blighe, P. E. Lyons, S. De, W. J. Blau, and J. N. Coleman, Carbon **46**, 41 (2008).
[13] N. M. Pugno, Nanotechnology **17**, 5480 (2006).
[14] N. M. Pugno, J. Phys.: Condens. Matter **19**, 395001 (2007).
[15] N. M. Pugno, J. Phys.: Condens. Matter **18**, S1971 (2006).
[16] N. M. Pugno, F. Bosia, and A. Carpinteri, Small **4**, 1044 (2008).
[17] F. Bosia, N. Pugno, G. Lacidogna, and A. Carpinteri, Int. J. Solids Struct. **45**, 5856 (2008).
[18] S. L. Phoenix, Int. J. Eng. Sci. **13**, 287 (1975).
[19] F. Kun, S. Zapperi, and H. J. Herrmann, Eur. Phys. J. B **17**, 269 (2000).
[20] R. C. Hidalgo, F. Kun, and H. J. Herrmann, Phys. Rev. E **64**, 066122 (2001).
[21] S. Pradhan, A. Hansen, and B. K. Chakrabarti, Rev. Mod. Phys. **82**, 499 (2010).
[22] S. L. Phoenix, Fibre Sci. Technol. **7**, 15 (1974).
[23] S. L. Phoenix and H. M. Taylor, Adv. Appl. Probab. **5**, 200 (1973).
[24] F. Raischel, F. Kun, and H. J. Herrmann, Phys. Rev. E **73**, 066101 (2006).
[25] H. E. Daniels, Adv. Appl. Probab. **21**, 315 (1989).
[26] M. C. Miguel and S. Zapperi, Science **312**, 1151 (2006).
[27] F. F. Csikor, C. Motz, D. Weygand, M. Zaiser, and S. Zapperi, Science **318**, 251 (2007).
[28] R. L. Smith and S. L. Phoenix, ASME Trans. J. Appl. Mech. **48**, 75 (1981).
[29] P. K. Porwal, I. J. Beyerlein, and S. L. Phoenix, J. Mech. Mater. Struct. **2**, 773 (2007).
[30] N. M. Pugno, Int. J. Fract. **140**, 159 (2006).
[31] N. Pugno, B. Peng, and H. D. Espinosa, Int. J. Solids Struct. **42**, 647 (2005).
[32] M. Ippolito, A. Mattoni, L. Colombo, and N. Pugno, Phys. Rev. B **73**, 104111 (2006).
[33] A. Carpinteri, F. Ciola, and N. Pugno, Comput. Struct. **79**, 389 (2001).
[34] S. L. Phoenix, M. Ibnabdeljalil, and C. Y. Hui, Int. J. Solids Struct. **34**, 545 (1997).
[35] W. I. Newman and S. L. Phoenix, Phys. Rev. E **63**, 021507 (2001).
[36] S. L. Phoenix and W. I. Newman, Phys. Rev. E **80**, 066115 (2009).
[37] D. C. Lagoudas, H. Chung-Yuen, and S. L. Phoenix, Int. J. Solids Struct. **25**, 45 (1989).
[38] D. D. Mason, C. Y. Hui, and S. L. Phoenix, Int. J. Solids Struct. **29**, 2829 (1992).
[39] I. J. Beyerlein, S. L. Phoenix, and R. Raj, Int. J. Solids Struct. **35**, 3177 (1998).
[40] A. Carpinteri, Int. J. Fract. **44**, 57 (1990).
[41] S. Pradhan and P. C. Hemmer, Phys. Rev. E **77**, 031138 (2008).
[42] S. Pradhan, A. Hansen, and P. C. Hemmer, Phys. Rev. Lett. **95**, 125501 (2005).
[43] N. Pugno, F. Bosia, A. S. Gliozzi, P. P. Delsanto, and A. Carpinteri, Phys. Rev. E **78**, 046103 (2008).